ChemComm

Accepted Manuscript

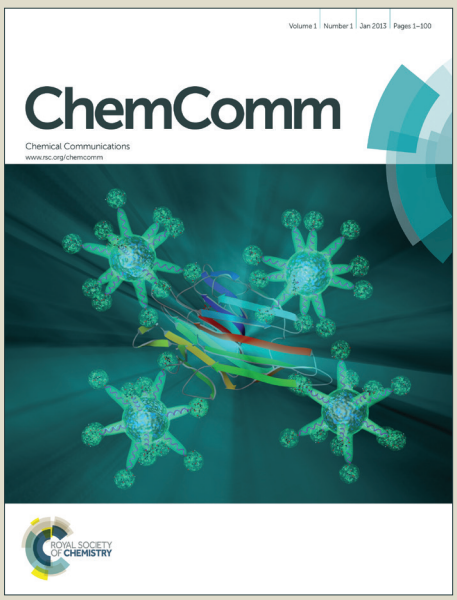

ROYAL SOCIETY OF CHEMISTRY

www.rsc.org/chemcomm

Journal Name

RSCPublishing

COMMUNICATION

A New Strategy to Construct FRET Platform for Ratiometric Sensing Hydrogen Sulfide

Cite this: DOI: 10.1039/xoxxoooooox

Longwei He,[a] Weiying Lin,*[a, b] Qiuyan Xu,[a] and Haipeng Wei [a]

Received ooth January 2012,
Accepted ooth January 2012

DOI: 10.1039/xoxxoooooox

www.rsc.org/

We introduce a new FRET strategy to construct a ratiometric fluorescent H_2S sensor. The ratio emission signal of coumarin-naphthalimide dyad is modulated by FRET process, which works in coordination with ICT mechanism. The FRET process on/off is controlled through tuning the overlap level of the donor emission spectrum with the acceptor absorption via modulation of acceptor fluorophore absorption wavelength. CN-N_3 was applied to visualize both the intracellular exogenous and endogenous H_2S through blue and green emission channels.

Fluorescence imaging has been widely used as a powerful tool for monitoring biomolecules within the context of living systems with high spatial and temporal resolution.[1] Researchers have constructed a large number of synthetic intensity-based fluorescent probes for bio-imaging.[2] However, the accuracy of the fluorescence imaging date is limited using intensity-based fluorescent probes, because many artificial environmental effects may influence the fluorescence intensity measurements, such as probe concentration, probe environment, and excitation intensity. Ratiometric fluorescent probes, on the contrary, can eliminate this shortcoming by self-calibration of two mission bands.[3]

Förster resonance energy transfer (FRET) is a nonradiative process in which an excited dye donor transfers energy to a dye acceptor in the ground state through long-range dipole–dipole interactions,[4] which is one of the most widely used sensing mechanisms for ratiometric fluorescent probes. Two requirements are necessary for FRET process occurring: (1) a substantial overlap of the donor emission spectrum with the acceptor absorption; (2) appropriate distance between the donor and acceptor (about 10 to 100 Å).[5] Therefore, generally FRET process on/off is controlled by modulation of acceptor molar absorption coefficient or tuning donor-acceptor distance.[6] As shown in Fig.1a, xanthene dyes (such as rhodamine and fluorescein) are the perfect model of molar absorption coefficient modulator because of their spirocyclization characteristics. They have relatively long absorption and emission wavelength and are usually used as acceptor fluorophores in FRET dyad. The fluorescent emission of xanthene-based dyes in the ring-closed form is inhibited and the FRET process of dyad is prohibited; whereas, after reaction with relevant analyte, ring-opened form displays strong absorption at around 550/480 nm (exclusive absorption of the rhodamine/fluorescein dye) and FRET process is existing. Another way for operating FRET process on/off is illustrated in Fig. 1b, when the donor and acceptor fluorophores are linked by an appropriate linker, FRET process of dyad occurs; whereas the linker is cut off by analyte and the distance between donor and acceptor gets extremely long, the FRET process will be prohibited. In addition to aforementioned two frequently-used strategies, there are of course special strategies to controlling FRET process. For example, Wagner's group used the quencher bleaching approach to activate FRET process by bio-specific or bio-orthogonal stimulus.[7]

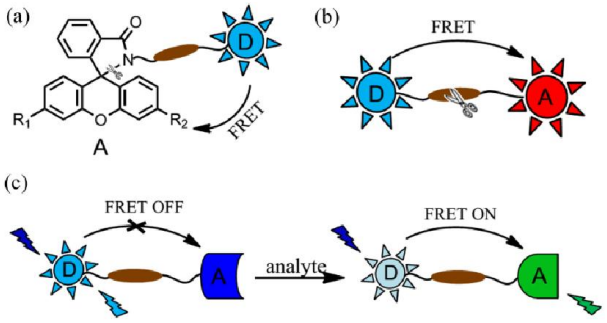

Fig. 1 Two known approaches (a, b) and our new strategy (c) to operate the dual emission bands of FRET dyad: (a) Modulation of acceptor molar absorption coefficient; (b) tuning donor-acceptor distance; (c) tuning the overlap level of the donor emission spectrum with the acceptor absorption via modulation of acceptor fluorophore absorption wavelength.

In this work, we have introduced a new strategy to construct ratiometric fluorescent probe based on FRET process. Different from two mentioned strategies, we changed the overlap level of the donor emission spectrum with the acceptor absorption via modulation of

acceptor fluorophore absorption wavelength to operate the FRET process on/off. On the one hand, we chose relatively short emission chromophore with high quantum yield as the energy donor; on the other hand, initial energy acceptor fluorophore has negligible overlap between the absorption spectrum and the donor emission, it displays nonfluorescent, however, reaction with relevant analyte would elicit absorption redshift and quantum yield increase via internal charge transfer (ICT) process. As shown in Fig. 1c, the new type of FRET dyad originally has negligible overlap of the donor emission spectrum with the acceptor absorption and FRET process is prohibited. The dyad displays donor dye emission. However, after reaction with relevant analyte, the absorption of acceptor fluorophore has a redshift and the quantum yield simultaneously increases induced by ICT process. It results that the degree of spectral overlap between the donor emission and the acceptor absorption gets a dramatic increase, meanwhile FRET process occurs. The dyad displays acceptor dye emission.

To examine the values of our new strategy, we have designed a ratiometric H_2S fluorescent sensor. Hydrogen sulfide has emerged as a member of the endogenous gaseous transmitter family of signaling molecules including nitric oxide (NO) and carbon monoxide (CO),[8] it also serves as an antioxidant or scavenger for reactive oxygen species (ROS).[9] However, abnormal levels of H_2S may induce many types of diseases, such as Alzheimer's disease, Down syndrome, and diabetes.[10] Therefore, detection of H_2S in living systems has attracted great attention and a large number of H_2S fluorescent probes have been reported recently.[11] Coumarin and naphthalimide dyes are the favorable building blocks for constructing fluorescent probes because of their excellent photophysical properties, such as high extinction coefficients, excellent quantum yields, and great photostability. What's more, the coumarin-naphthalimide dyad is an ideal FRET platform as the emission spectrum of coumarin well overlaps with the naphthalimide absorption.[12] Azido group is well-known for sensitive and selective response to H_2S. What's more, the azido derivatives could be specifically reduced by H_2S affording the amino products, it usually results in absorption redshift and emission enhancement via ICT process.[11b-e, 13] Thus, we chose 7-diethylamino coumarin and 4-azido-1,8-naphthalimide naphthalimide as two moiety of the new type of FRET dyad (**CN-N_3**) (Scheme 1). The supposed ratiometric fluorescence mechanism of **CN-N_3** interacts with H_2S and according reduced product **CN-NH_2** are also shown in Scheme 1. Prior to react with H_2S, we supposed that probe **CN-N_3** has negligible overlap of the coumarin emission spectrum with the naphthalimide azide absorption and FRET process does not exist

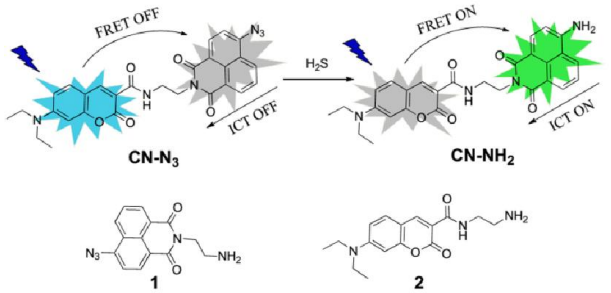

Scheme 1 A proposed novel ratiometric fluorescent H_2S probe based on the new FRET strategy and structures of control compounds **1** and **2**.

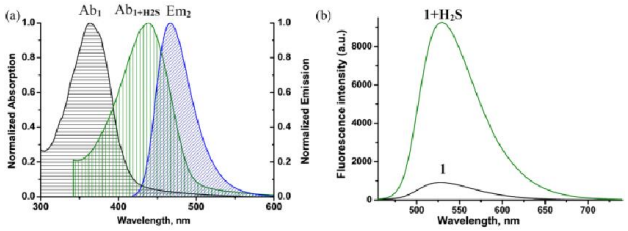

Fig. 2 (a) The normalized absorption spectra of control compound **1** before (black horizontal) and after (green vertical) addition of NaHS and normalized fluorescence spectrum of control compound **2** (blue oblique). (b) The fluorescence spectra of **1** in the absence (black) and presence (green) of H_2S in ethanol.

(Fig. 2a). The dyad displays coumarin emission. However, interaction of naphthalimide azide with H_2S affords 4-amino-1,8-naphthalimide, which elicits absorption redshift and fluorescence intensity increase via ICT process caused by the electron donating amine and the electron withdrawing imide (Fig. 2a-b). It results **CN-NH_2** has a significant overlap of the emission spectrum of coumarin with the naphthalimide absorption and FRET process occurs. The dyad displays naphthalimide fluorescence (Scheme 1). Thus, the dyad **CN-N_3** might detect H_2S as a ratiometric fluorescent sensor based on the new FRET strategy.

The target compound **CN-N_3** was readily synthesized in one simple step as shown in Scheme 2. Treatment of compound **3** with sodium azide in dry DMF afforded dyad **CN-N_3** in good yield. The control compounds **1** and **2** were also prepared (See ESI†). The structures of the compounds synthesized were fully characterized by the standard NMR and mass spectrometry (See ESI†).

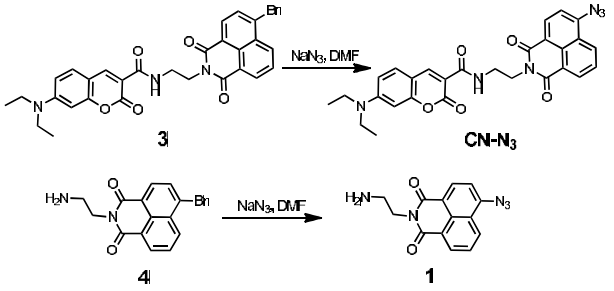

Scheme 2 Synthesis of H_2S sensor **CN-N_3** and control compound **1.**

With compound **CN-N_3** in hand, we first evaluated the capability of **CN-N_3** to detect H_2S in aqueous buffer. The titration of H_2S to the probe **CN-N_3** was performed in 25 mM PBS buffer (pH 7.4) with 50% ethanol. As designed, upon excitation at 408 nm, the free sensor only displayed the characteristic emission peak of the coumarin donor at around 474 nm but no featured emission band of the naphthalimide moiety (Fig. 3a). However, addition of NaHS (a standard source for hydrogen sulfide) elicited the formation of a significant naphthalimide acceptor emission peak at around 534 nm and simultaneously the emission peak of coumarin donor gradually disappeared (Fig. 3a), suggesting that **CN-N_3** was reduced affording **CN-NH_2** in the presence of H_2S and FRET from the coumarin unit to the naphthalimide moiety was effectively induced by ICT effect. This observation indicated the sensing mechanism of **CN-N_3** is an integration of ICT and FRET mechanisms (Scheme 1). The ratios of fluorescence intensities at 534 and 474 nm (I_{534}/I_{474}) exhibit 8.7-fold

increase. Importantly, the chemodosimeter shows an excellent linear relationship between the emission ratios and the concentrations of H_2S from 1.0 μM to 30 μM (Fig. 3b), suggesting that the chemodosimeter is potentially useful for quantitative determination of H_2S. The changes in the absorption spectra are in good agreement with the variations in the emission profile. As shown in Fig. S1 (ESI†), upon addition of H_2S, the absorption of naphthalimide azide at around 364 nm gradually faded and simultaneously a new red-shifted (61 nm) absorption band at around 425 nm (characteristic absorption of amino naphthalimide) was enhanced.

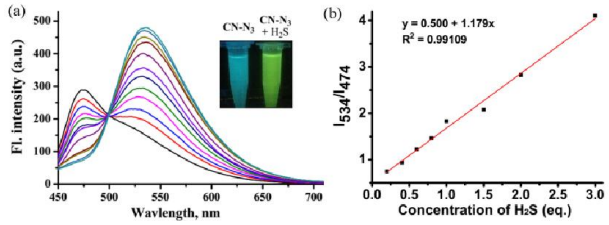

Fig. 3 (a) Fluorescence spectra (λ_{ex}= 408 nm) of 10 μM **CN-N$_3$** with 0–5.0 eq. of NaHS in 25 mM phosphate buffer (pH 7.4, containing 50% ethanol). The inset shows the visual fluorescence color of **CN-N$_3$** before (left) and after (right) addition of H_2S (UV lamp, 365 nm). (b) The linear relationship between the fluorescence intensity ratio (I_{534}/I_{474}) and the concentration of H_2S.

To shed light on the H_2S-triggered fluorescence ratio response, we decided to characterize the reduced product. Incubation of **CN-N$_3$** with NaHS afforded the product **CN-NH$_2$**, which isolated and characterized by standard NMR and mass spectrometry (Fig. S2-4, ESI†). These experimental facts support our proposed switching mechanism.

The detection limit was calculated to be 9.1×10^{-8} M (S/N = 3), indicating that the probe is highly sensitive to H_2S. To examine the selectivity, the probe **CN-N$_3$** (10 μM) was treated with various biologically relevant species (e.g., the representative anions, reactive oxygen species, reducing agents, small-molecule thiols, and NaHS) in the aqueous buffer. As exhibited in Fig. 4, addition of the representative interfering species including Cl^-, F^-, CO_3^{2-}, HCO_3^-, SO_4^{2-}, HPO_4^{2-}, NO_2^-, Ac^-, citrate at 1 mM, and $S_2O_3^{2-}$, ClO^-, H_2O_2 at 200 μM induced no marked ratio increase. Notably, small-molecule thiols such as glutathione (GSH) and cysteine at 5 mM triggered

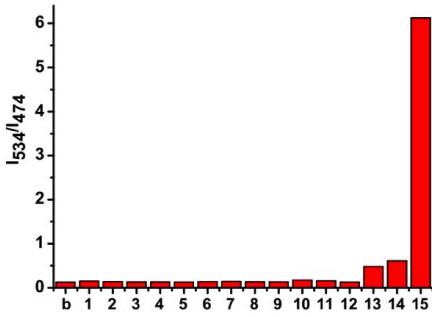

Fig. 4 Ratios of fluorescence intensity (I_{534}/I_{474}) of sensor **CN-N$_3$** (10 μM) in the presence of various analytes in aqueous solution (pH 7.4 PBS, containing 50% ethanol): b, blank; 1, Cl^-; 2, F^-; 3, CO_3^{2-}; 4, HCO_3^-; 5, SO_4^{2-}; 6, HPO_4^{2-}; 7, $S_2SO_3^{2-}$; 8, NO_2^-; 9, Ac^-; 10, citrate; 11, ClO^-; 12, H_2O_2; 13, Cys; 14, GSH; 15, NaHS.

only a small ratio increase. However, just addition of 20 μM NaHS can elicit obvious increase of ratio value (I_{534}/I_{474}). The ratio value reached its maximum at about 2.5 min (Fig. S5, ESI†). The results suggested probe **CN-N$_3$** has a high selectivity for H_2S over other biological species. What's more, increase of fluorescence signal ratios was observed at round physiological pH (Fig. S6, ESI†), and the probe **CN-N$_3$** has little cytotoxicity for living cells (Fig. S7, ESI†). The results indicated **CN-N$_3$** may be suitable for studies of H_2S in the living systems.

We then examined where probe **CN-N$_3$** is located in living cells. PC-3 cells were co-stained with the probe and LysoTracker Red (a commercial lysosome probe) or Mitotracker Red FM (a commercial mitochondrial probe), respectively. As shown in Fig. S8 (ESI†), the merged confocal fluorescence images of **CN-N$_3$** and commercial cellular organelle-specific probes did not overlap well (Pearson's co-localization coefficient 0.56 for lysosome and 0.66 for mitochondria). These results suggested that the probe is not predominately located in these organelles, but in the cytoplasm. We then proceeded to examine the ability of the sensor for monitoring H_2S in living cells. For proof-of-concept, **CN-N$_3$** (5 μM) was initially incubated with PC-3 cells for 20 min, and then treated with 20 μM NaHS. The cells incubated with only the sensor **CN-N$_3$** displayed strong fluorescence in the blue channel (Fig. 5a) and faint fluorescence in the green channel (Fig. 5b). However, the cells loaded with both the sensor **CN-N$_3$** and NaHS exhibited gave intense green fluorescence (Fig. 5f) but very faint blue fluorescence (Fig. 5e), indicating that intracellular **CN-N$_3$** was reduced by H_2S affording **CN-NH$_2$**. The ratiometric fluorescence images were acquired using commercial software (Image-Pro Plus) and are shown in Fig. 5c and g, the ratios of emission intensity (green/blue) got a significant increase after addition of NaHS. Thus, these results reveal that **CN-N$_3$** is cell membrane permeable and capable of sensing H_2S in living cells.

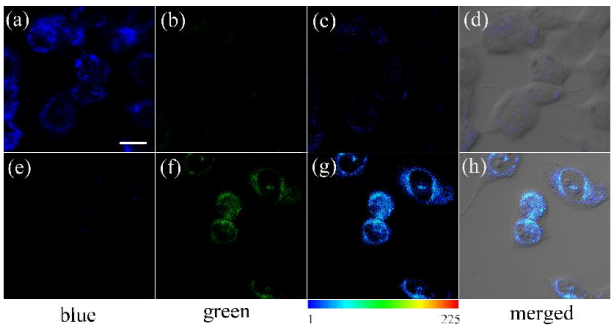

Fig. 5 Confocal fluorescence images of PC-3 cells incubated with 5 μM **CN-N$_3$** for 20 min (a-c) and then 20 μM NaHS for 10 min (e-g). Images were acquired using 405 nm excitation and emission channels of (a, e) 450−480 nm (blue) and (b, f) 520−560 nm (green); (c, g) ratio images of green to blue channel; (d, h) merged bright field and ratio images. Scale bar = 20 μm.

In addition to image extraneous H_2S, we determine to detect intrinsically biosynthesis H_2S inside the cells. Cysteine could be catalyzed by cystathionine β-synthase (CBS) and cystathionine γ-lyase (CSE) in living cells for H_2S production.[12] PC-3 cells were incubated with 200 μM cysteine for 1 hour, followed addition of 5 μM **CN-N$_3$**. As shown in Fig. 6, in the absence of cysteine, the cells displayed strong fluorescence in the blue channel and faint

fluorescence in the green channel. However, the cells incubated cysteine induced a fluorescent emission decrease in blue channel (Fig. 6e) and significant emission increase in green channel (Fig. 6f). The ratios of emission intensity (green/blue) got a marked increase in the presence of cysteine (Fig. 6g). These results further indicate that **CN-N$_3$** is capable of detecting not only external H_2S in living cells, but also H_2S biologically produced by the cells.

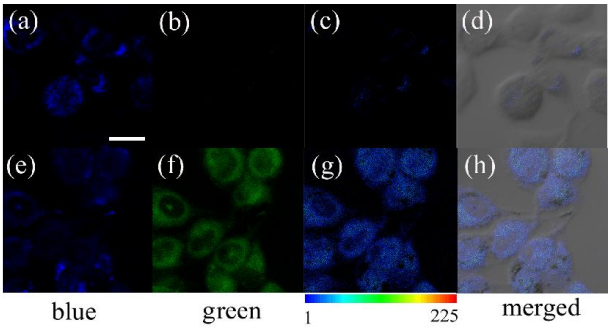

Fig. 6 Confocal fluorescence images of PC-3 cells incubated with 5 μM **CN-N$_3$** only for 20 min (a-c) and 200 μM cystine for 1 hour followed by 5 μM **CN-N$_3$** for 20 min (e-g). Images were acquired using 405 nm excitation and emission channels of (a, e) 450−480 nm (blue) and (b, f) 520−560 nm (green); (c, g) ratio images of green to blue channel; (d, h) merged bright field and ratio images. Scale bar = 20 μm.

In summary, we have introduced a new FRET strategy to construct a ratiometric fluorescent H_2S sensor. The FRET mechanism of **CN-N$_3$** interacting with H_2S works in coordination with ICT process, the ratio signals are modulated through tuning the overlap level of the donor emission spectrum with the acceptor absorption via modulation of acceptor fluorophore absorption wavelength. The sensor exhibited clear dual-emission signal changes in blue and green spectral windows upon H_2S level changes. We have demonstrated that the sensor is suitable for measuring cellular H_2S, but also for monitoring both the exogenous and endogenous H_2S in living cells.

This work was financially supported by NSFC (21172063, 21472067) and the startup fund of University of Jinan.

Notes and references

[a] State Key Laboratory of Chemo/Biosensing and Chemometrics, College of Chemistry and Chemical Engineering, Hunan University, Changsha, Hunan 410082, China.

[b] Institute of Fluorescent Probes for Biological Imaging, School of Chemistry and Chemical Engineering, School of Biological Science and Technology, University of Jinan, Jinan, Shandong 250022, P.R. China. E-mail: weiyinglin2013@163.com.

† Electronic Supplementary Information (ESI) available: [Experimental procedures, characterization data, and additional spectra]. See DOI: 10.1039/c000000x/

1 (a) T. Ueno, T. Nagano, *Nat. Methods*, 2011, **8**, 642; (b) H. Kobayashi, M. Ogawa, R. Alford, P. L. Choyke, Y. Urano, *Chem. Rev.,* 2010, **110**, 2620.

2 (a) H. Zheng, X. Zhan, Q. Bian and X. Zhang, *Chem. Commun.*, 2013, **49**, 429; (b) Y. Yang, Q. Zhao, W. Feng and Fuyou Li, *Chem. Rev.*, 2013, **113**, 192; (c) Z. Yang, J. Cao, Y. He, J. H. Yang, T. Kim, X. Peng and J. S. Kim, *Chem. Soc. Rev.*, 2014, **43**, 4563; (d) Z. Guo, S. Park, J. Yoon and I. Shin, *Chem. Soc. Rev.*, 2014, **43**,16.

3 (a) A. P. Demchenko, *J Fluoresc.*, 2010, **20**, 1099; (b) K. Kikuchi, H. Takakusa, T. Nagano, *Trend. Anal. Chem.*, 2004, **23**, 407.

4 K. E. Sapsford, L. Berti, and I. L. Medintz, *Angew. Chem., Int. Ed.*, 2006, **45**, 4562.

5 C. G. dos Remedios and P. D. J. Moens, *J. Struct. Biol.*, 1995, **115**, 175.

6 (a) J. Fan, M. Hu, P. Zhan and X. Peng, *Chem. Soc. Rev.,* 2013, **42**, 29; (b) L. Yuan, W. Lin, K. Zheng, and S. Zhu, *Acc. Chem. Res.*, 2013, **46**, 1462, (c) B. Chen, P. Wang, Q. Jin and X. Tang, *Org. Biomol. Chem.*, 2014, **12**, 5629.

7 C. Egloff, S. A. Jacques, M. Nothisen, D. Weltin, C. Calligaro, M. Mosser, J.-S. Remy and A. Wagner, *Chem. Commun.*, 2014, **50**, 10049.

8 (a) E. Culotta and D. E. Koshland Jr, *Science*, 1992, **258**, 1862; (b) Y. Han, J. Qin, X. Chang, Z. Yang and J. Du, *Cell. Mol. Neurobiol.*, 2006, **26**, 101.

9 H. Mitsuhashi, H. Ikeuchi, Y. Nojima, *Clin. Chem.*, 2001, **47**, 1872.

10 (a) K. Eto, T. Asada, K. Arima, T. Makifuchi and H. Kimura, Biochem, *Biophys. Res. Commun.*, 2002, **293**, 1485; (b) P. Kamoun, M.-C. Belardinelli, A. Chabli, K. Lallouchi and B. Chadefaux-Vekemans, *Am. J. Med. Genet.*, 2003, **116A**, 310; (c) W. Yang, G. Yang, X. Jia, L. Wu and R. Wang, *J. Physiol.*, 2005, **569**, 519.

11 (a) F. Yu, X. Han and L. Chen, *Chem. Commun.*, 2014, **50**, 12234; (b) N. Adarsh, M. S. Krishnan, D. Ramaiah, *Anal. Chem.*, 2014, **86**, 9335; (c) Y. Cai, L. Li, Z. Wang, J. Z. Sun, A. Qin and B. Z. Tang, *Chem. Commun.*, 2014, **50**, 8892; (d) Q. Qiao, M. Zhao, H. Lang, D. Mao, J. Cui and Z. Xu, *RSC Adv.*, 2014, **4**, 25790; (e) C. Wei, R. Wang, L. Wei, L. Cheng, Z. Li, Z. Xi and L. Yi, *Chem. Asian J.*, DOI: 10.1002/asia.201402808; (f) X. L. Liu, X. J. Du, C. G. Dai and Q. H. Song, *J. Org. Chem.*, 2014, **79**, 9481; (g) X. J. Zou, Y. C. Ma, L. E Guo, W. X. Liu, M. J. Liu, C. G. Zou, Y. Zhou and J. F. Zhang, *Chem. Commun.*, 2014, **50**, 13833; (h) X. Wang, J. Sun, W. Zhang, X. Ma, J. Lv and B. Tang, *Chem. Sci.*, 2013, **4**, 2551; (i) M. Strianese, G. J. Palm, S. Milione, O. Kühl, W. Hinrichs and C. Pellecchia, *Inorg. Chem.*, 2012, **51**, 11220; (j) M. Strianese, F. De Martino, C. Pellecchia, G. Ruggiero, S. D'Auria, *Protein. Pept. Lett.*, 2011, **18**, 282.

12 X. Zhou, F. Su, H. Lu, P. Senechal-Willis, Y. Tian, R. H. Johnson and D. R. Meldrum, *Biomaterials*, 2012, **33**, 171.

13 (a) T. Ozdemir, F. Sozmen, S. Mamur, T. Tekinay and E. U. Akkaya, *Chem. Commun.*, 2014, **50**, 5455; (b) W. Sun, J. Fan, C. Hu, J. Cao, H. Zhang, X. Xiong, J. Wang, S. Cui, S. Sun and X. Peng, *Chem. Commun.*, 2013, **49**, 3890; (c) F. Yu, P. Li, P. Song, B. Wang, J. Zhao and K. Han, *Chem. Commun.*, 2012, **48**, 2852; (d) Q. Wan, Y. Song, Z. Li, X. Gao and H. Ma, *Chem. Commun.*, 2013, **49**, 502; (e) G. Mao, T. Wei, X. Wang, S. Huan, D. Lu, J. Zhang, X. Zhang, W. Tan, G. Shen and R. Yu, *Anal. Chem.*, 2013, **85**, 7875; (f) Leticia A. Montoya and Michael D. Pluth, *Chem. Commun.*, 2012, **48**, 4767.

14 (a) Y. Qian, J. Karpus, O. Kabil, S. Y. Zhang, H. L. Zhu, R. Banerjee, J. Zhao and C. He, *Nat. Commun.*, 2011, **2**, 495; (b) S. Yang, Y. Qi, C. Liu, Y. Wang, Y. Zhao, L. Wang, J. Li, W. Tan and R. Yang, *Anal. Chem.*, 2014, **86**, 7508.